SUPPLEMENTAL MATERIALS

AIP1 functions as an endogenous inhibitor of VEGFR2-mediated signaling and inflammatory angiogenesis

Haifeng Zhang[1*], Yun He[1*], Shengchuan Dai[1*], Zhe Xu[2*], Yan Luo[2], Ting Wan[2], Dianhong Luo[1], Dennis Jones[1], Shibo Tang[2], Hong Chen[1], William C. Sessa[1], and Wang Min[1,3]

[1]Interdepartmental Program in Vascular Biology and Therapeutics, Department of Pathology, Yale University School of Medicine, 10 Amistad St., New Haven, CT 06520. [2]Zhongshan Ophthalmic Center, Sun Yat-Sen University, Guangzhou, P.R. China.

[3]Corresponding author: Dr. Wang Min, Interdepartmental Program in Vascular Biology and Transplantation and Department of Pathology, Yale University School of Medicine, 10 Amistad St., New Haven, CT 06520.
Tel: 203-785-6047; Fax: 203-737-2293; Email: wang.min@yale.edu

[*]These authors contributed equally to this work.

Fig.S1

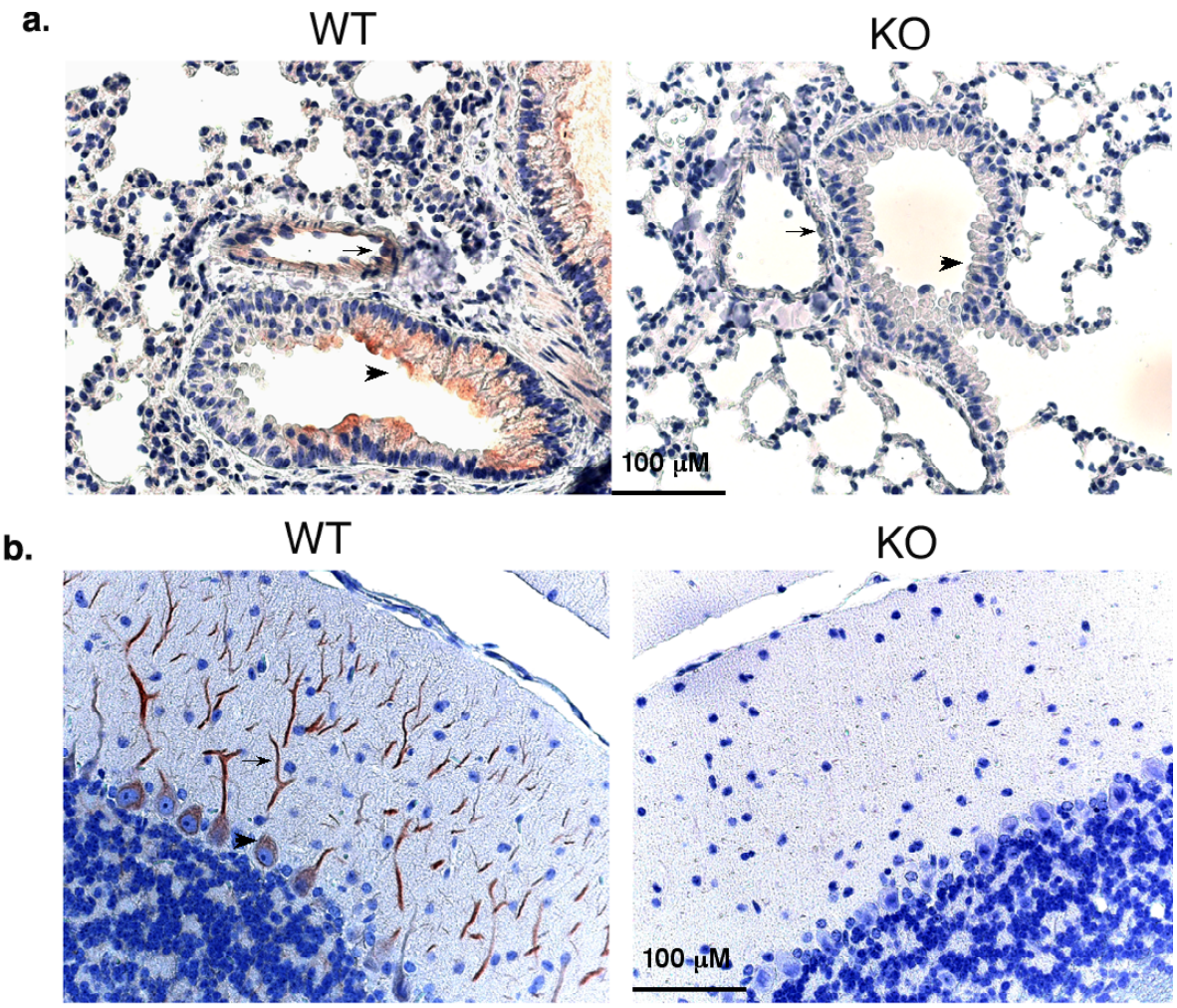

Fig.S1. AIP1 deletion in tissues. **a**. AIP1 expression in paraffin section of lung (**a**) and brain (**b**) was determined by immunohistochemistry with anti-AIP1. Arrow indicates vascular endothelium and arrowhead for lung bronchial epithelium. **b**: Arrow indicates axon and arrowhead for cell body of a purkinjie cell.

Fig.S2

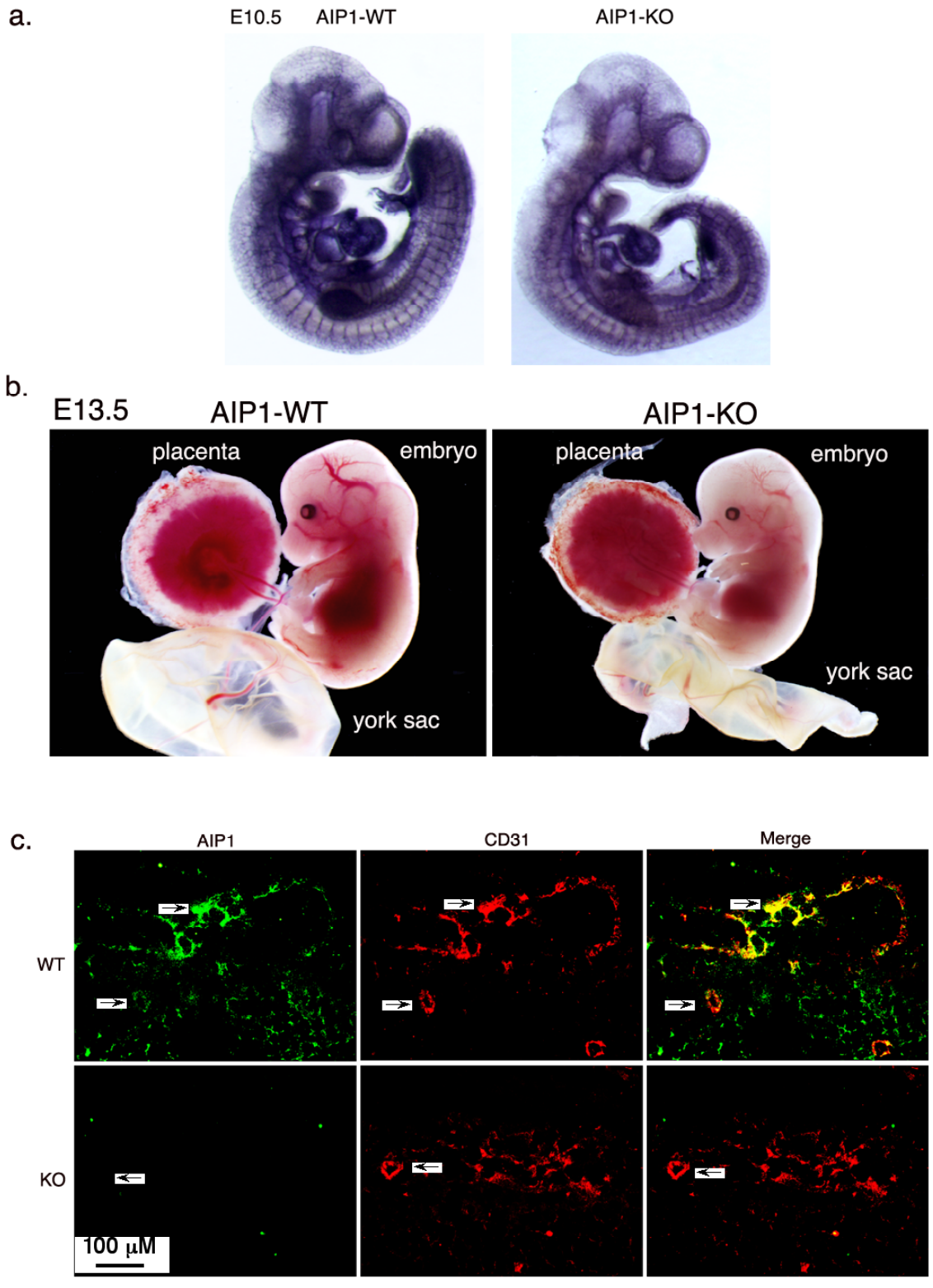
a.
E10.5
AIP1-WT
AIP1-KO
b.
E13.5
AIP1-WT
AIP1-KO
placenta
embryo
york sac
placenta
embryo
york sac
c.
AIP1
CD31
Merge
WT
KO
100 μM

Fig.S2. AIP1 expression in vasculature during embryogenesis and effects of AIP1 deletion on vascular development. **a-b**. Effects of AIP1 deletion on vascular development. AIP1-WT and AIP1-KO embryos were obtained by mating AIP1+/- mice and embryos were harvested at indicated times (E9.5-E16.5). For E9.5-11.5 embryos, embryo vasculature was visualized by whole mount-staining with anti-CD31 antibody. Shown images in **a** are E10.5 embryos. For E13.5-16.5 embryos, freshly dissected embryos without staining were photographed. Shown images in **b** are E13.5 embryo, york sac and placenta. **c**. AIP1 expression in vasculature during development. E13.5 embryos were co-stained by immunostaining with anti-AIP1 (rabbit) and anti-CD31 (an EC marker, goat) antibodies followed FITC-conjugated secondary antibody against rabbit IgG and phycoerythrin (PE)-conjugated secondary antibody against goat IgG. Images were taken under fluorescence microscope. Co-localization of AIP1 with CD31 is detected in AIP1-WT but not AIP1-KO mice (indicated by arrows).

Fig.S3

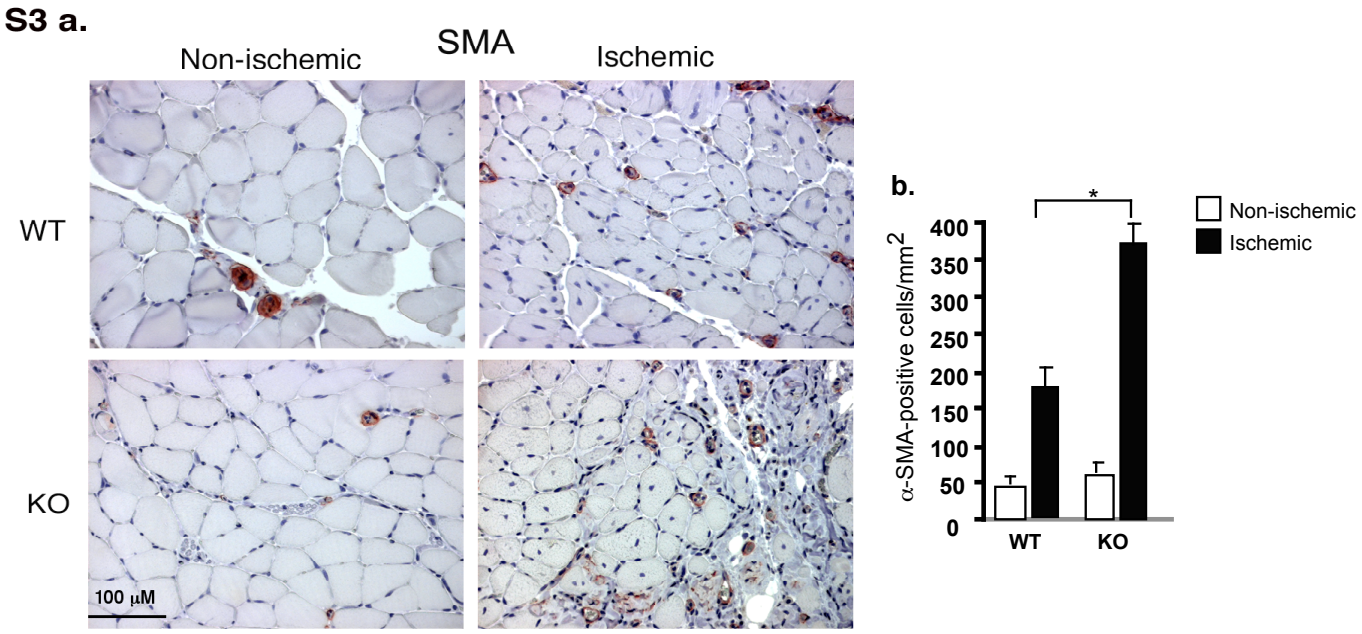

Fig.S3. AIP1-KO mice showed enhanced vessel maturation. Pericyte/smooth muscle cells were immunostained with smooth muscle α-actin (SMA, a smooth muscle/pericyte marker). Representative sections from non-ischemic and ischemic groups of AIP1-WT and AIP1-KO mice on day 28 post-ischemia are shown in **a**. Quantification of SMA-positive capillaries (number/mm^2 muscle area) are shown. Data are mean ± SEM from 10 fields per section (3 sections/mouse and n=4 for each strain). *, $p<0.05$.

Fig.S4

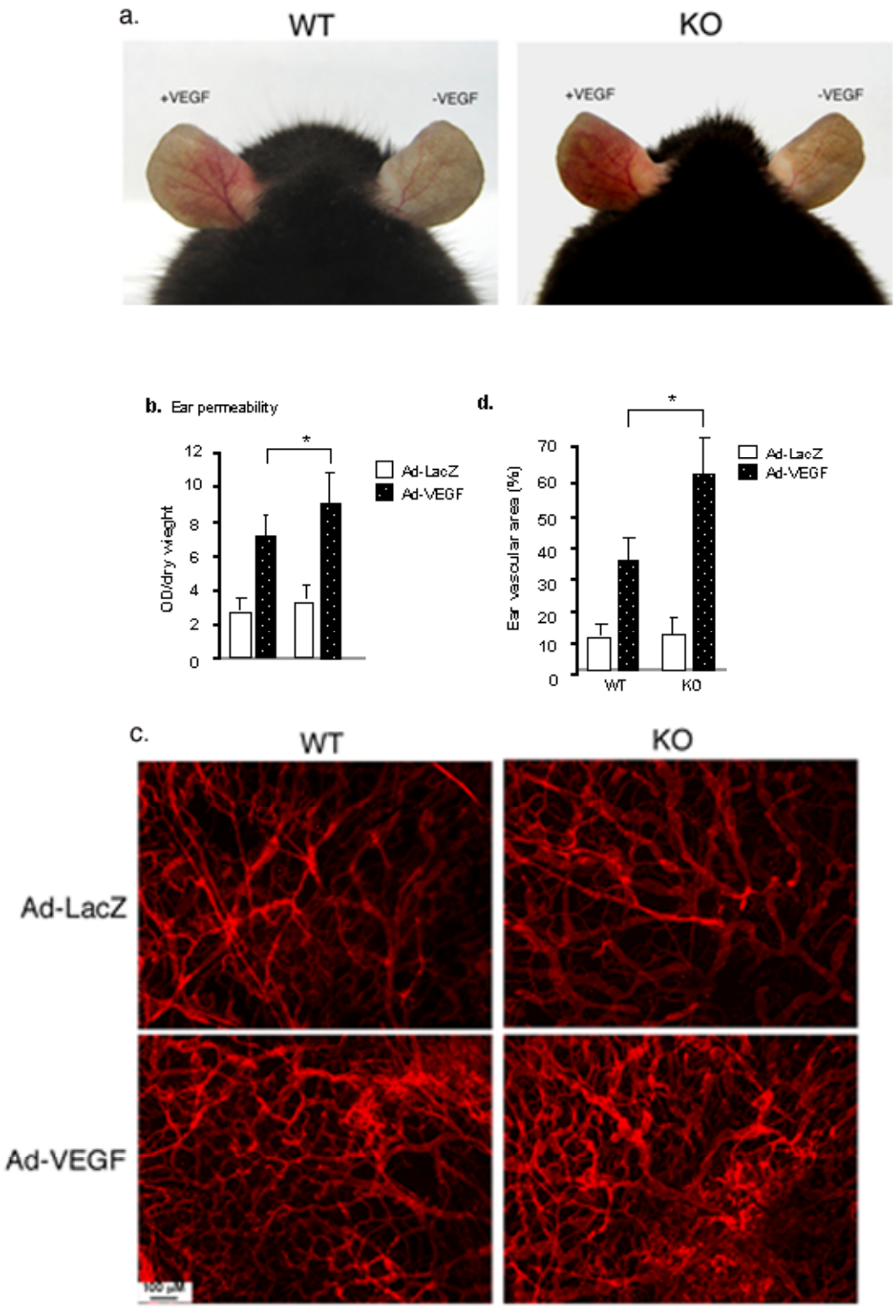
a.
WT
KO
+VEGF
-VEGF
+VEGF
-VEGF
b. Ear permeability
OD/dry wieght
12
10
8
6
4
2
0
*
Ad-LacZ
Ad-VEGF
d.
Ear vascular area (%)
70
60
50
40
30
20
10
0
*
Ad-LacZ
Ad-VEGF
WT
KO
c.
WT
KO
Ad-LacZ
Ad-VEGF

Fig.S4. VEGF-induced ear neovascularization was greatly augmented in AIP1-KO mice. VEGF-induced ear angiogenesis. Adenovirus encoding $VEGF_{164}$ ($1x10^9$ pfu) (Ad-VEGF) or β-galactosidase (Ad-LacZ) was intradermally injected into the mice right and left ear skin, respectively. **a**. VEGF-induced angiogenesis in AIP1-WT and AIP1-KO mice was accessed by a direct microscopy. **b**. Ear permeability was measured by Evan's blue dye (EBD) assay. Ear skin containing the extravasated protein-bound dye was excised and the dye was extracted from the tissue. Dye concentrations were measured at 630 nm using a spectrophotometer. The values obtained are expressed as total nanograms of EBD extracted, and are a measure of the total amount of protein-bound dye that extravasated in response to adenoviral-expressed VEGF or LacZ. Data are expressed as mean ± SEM from n=3 for each strain. *, $p<0.05$. **c**. Ear vasculature was visualized by a whole-mount staining with PE-conjugated anti-CD31. **d**. Quantification of vessel density from **c**. Data are mean ± SEM from 10 fields per ear (n=5 for each group). *, $p<0.05$.

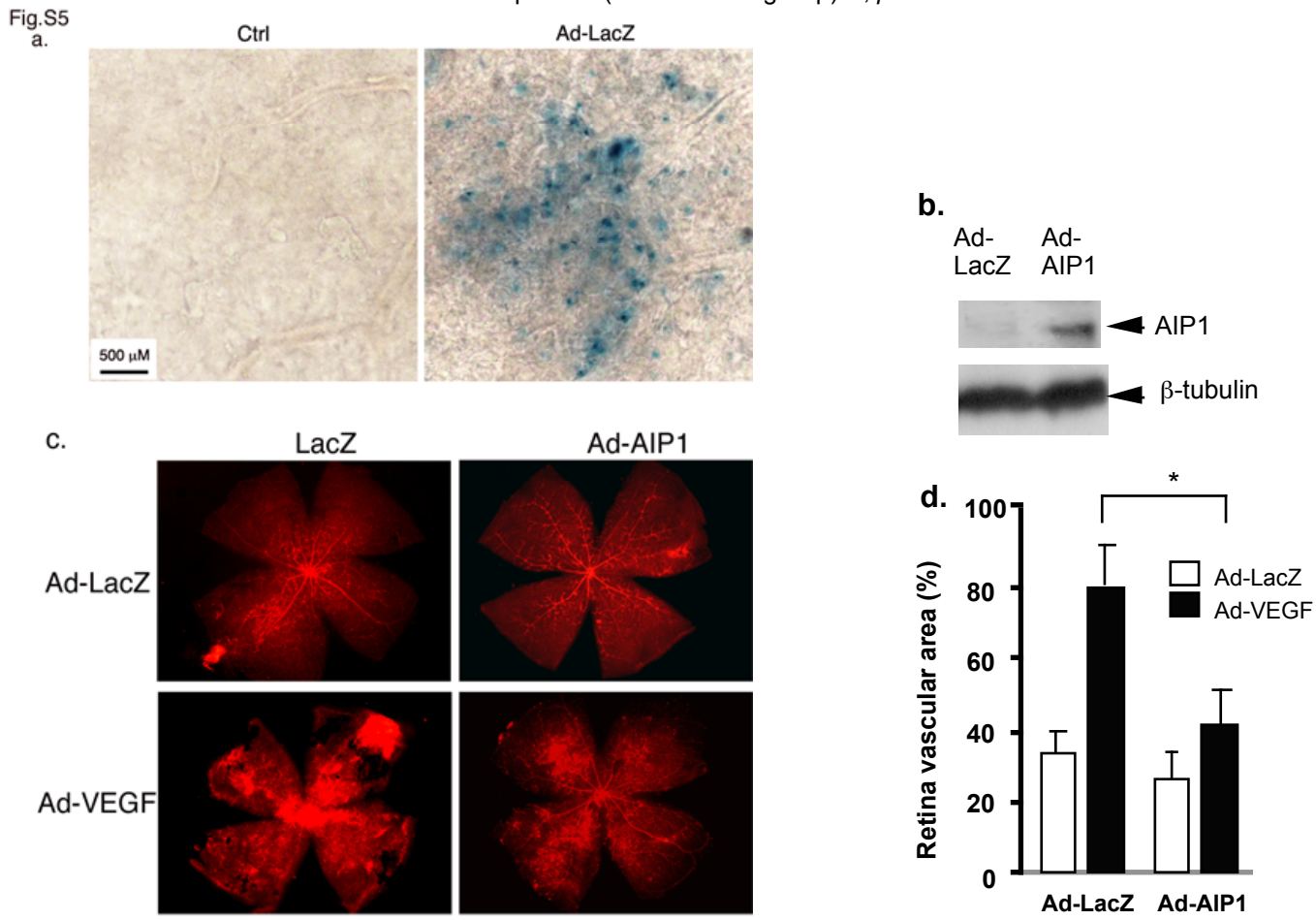

Fig.S5. Overexpression of AIP1 inhibits VEGF-induced in vivo angiogenesis. a-b. Transgene expression of LacZ reporter and AIP1. Ad-LacZ or Ad-AIP1 ($2x10^8$ pfu) was injected intravetrously into AIP1-KO mice. LacZ expression in retina was visualized by β-galactosidase staining (**a**) and AIP1 expression was detected by Western blot with anti-AIP1 (**b**). **c-d**. AIP1 expression inhibits VEGF-induced retina angiogenesis. Ad-AIP1 or Ad-LacZ was co-ministrated intravetrously into AIP1-KO mice. Retina vasculature was visualized by isolectin staining (**c**) with quantification of vessel density in **d**. Data are mean ± SEM from 10 fields per retina (n=4 for each group). *, $p<0.05$.

Fig.S6

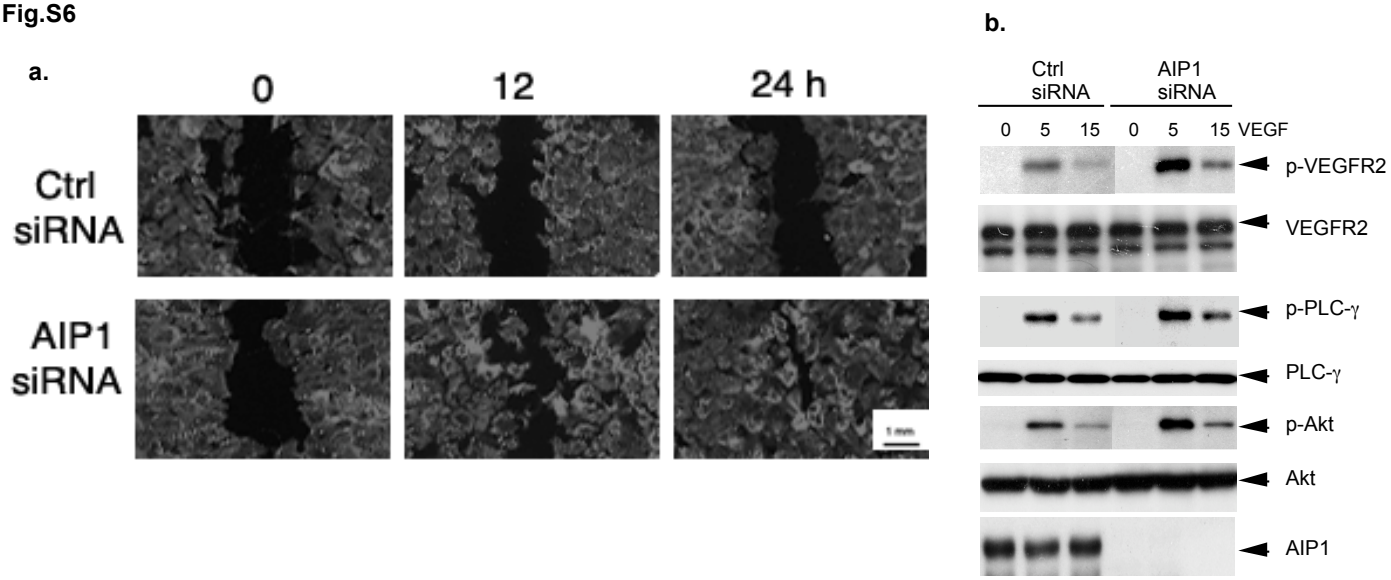

Fig.S6. VEGF-induced EC migration and signaling are augmented by AIP1 knockdown. HUVEC were transfected with control siRNA or AIP1 siRNA oligonucleotides. 36 h post-transfection, cells were starved for 12 h. **a**. AIP1 knockdown increases VEGF-induced EC migration. Cells were subjected to a monolayer "wound injury" assay as described in **Fig.5** in the presence of VEGF (10 ng/ml) for indicated times. Data presented are means (±SEM) of the triplicates from three independent experiments. **b**. AIP1 knockdown increases VEGF-induced VEGFR2 activation. Cells were treated with VEGF (10 ng/ml) for 5 min. Phosphorylation of VEGFR2, total VEGFR2, AIP1 and β-tubulin were determined by Western blot with respective antibodies.

Fig.S7 MLEC

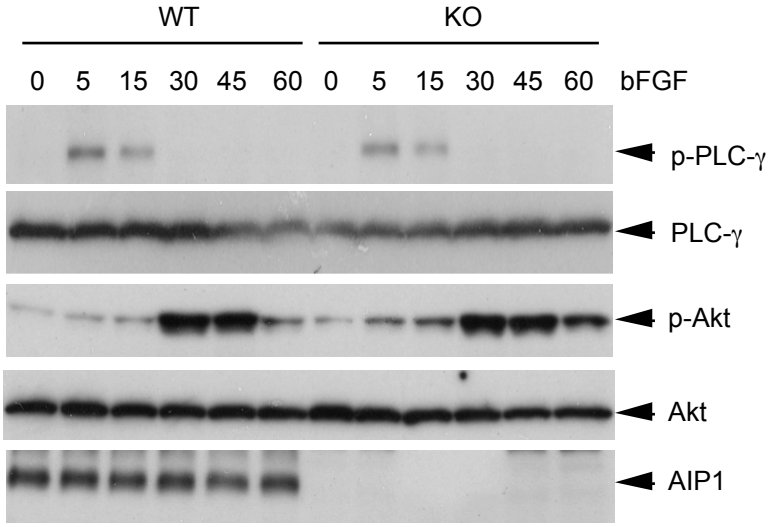

Fig.S8 Muscle

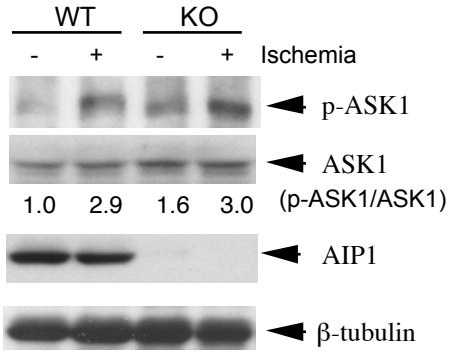

Fig.S7. AIP1 deletion has no effect on bFGF signaling in cultured EC. AIP1-WT and AIP1-KO MLEC were cultured overnight in 0.5% FBS followed by bFGF treatment (10 ng/ml) for indicated times (0-60 min). Phosphorylation of PLC-γ and Akt were determined by Western blot with phospho-specific antibodies. Total PLC-γ and Akt as well as AIP1 were determined by Western blot with respective antibodies.

Fig.S8. AIP1 deletion has no effect on ischemia-induced ASK1-JNK signaling in tissue. AIP1-WT and AIP1-KO were subjected to ischemic ligation, and tissues were harvested on day 7. Activation of ASK1 was determined by Western blot with a phospho-specific antibody (pThr845). Relative ratios of p-ASK1/ASK1 are shown, with untreated WT as 1.0. As controls, AIP1 and β-tubulin proteins were also determined.